AN EXPERIMENTAL STUDY ON THE DEVELOPMENT OF GAS-LIQUID SLUG FLOWS WITH DIRECTION CHANGE

Victor Enrique Llantoy Parra
Cristiane Cozin
Fausto Arinos de Almeida Barbuto
LACIT/PPGEM/UTFPR, Curitiba, Paraná, Brazil
victorllantoy@gmail.com
cozin@utfpr.edu.br
fbarbuto@utfpr.edu.br

Carlos A. F. Amaral
Marco José da Silva
CPGEI/UTFPR, Curitiba, Paraná, Brazil
ceamaral@hotmail.com
mdasilva@utfpr.edu.br

Rigoberto E. M. Morales
LACIT/PPGEM/UTFPR, Curitiba, Paraná, Brazil
rmorales@utfpr.edu.br

Abstract. *Slug flow is the most common flow pattern occurring in the transportation of gas-liquid two-phase mixtures in pipes. This flow pattern is characterized by the alternation of liquid slugs and elongated bubbles whose lengths and velocities change in space and time. Slight direction changes in pipe inclination make these liquid slugs to grow or, quite often, generate new ones by bubble break-up. Other phenomena, as deceitful as intriguing and fascinating, may happen upon the change in direction at some specific in situ liquid and gas flow rate combinations. Briefly stated, slug flow is rather complex pattern worthy of a careful and detailed study. An experimental work aimed at capturing the essence of these flows and their physical behaviour was carried out. A transparent, 1-inch OD pipe with 9 metres of length and a direction change of 7 degrees upward was used to carry an air-water mixture at different flow rates, all within the slug flow occurrence zone. Four probing stations with parallel resistive wire sensors were installed at pre-defined positions along the pipe. The objective of these sensors was to measure important flow parameters such as the bubble and slug lengths velocities and lengths and the gas and liquid volume fractions. High speed cameras to capture the whole transit of the slug units were positioned at two observation stations, one at a horizontal section and another at the very point where direction change occurred. The images captured by this camera brought out misleading behaviours that signal processing alone could not explain. Data signals from the experiment were recorded to large mass storage media, thus building a quite extensive data base. The PDF technique was used to analyze the flow data, revealing peculiar and noteworthy results.*

Keywords: *Gas-liquid slug flows, direction change, bubble break-up, experimental data, statistical analysis.*

1. INTRODUCTION

Gas-liquid slug flows are found in several industrial applications such as the production and transportation of crude oil and associated gas mixtures, steam generation in nuclear and fossil power plants, evaporators and condensers, distillation units, boilers and so forth. These flows possess an intermittent behaviour and are characterized by the alternate succession of two distinct bodies or regions: the *liquid slug* and the *elongated bubble*. Together, those two regions form that what is usually known as a slug unit cell or, simply put, the *unit cell*.

An overabundance of researchers has dedicated their time and efforts to better understand and describe the behaviour of such gas-liquid flow regime. Earlier models described slug flows as a stationary phenomenon inasmuch as the required computational power to accurately tackle the slug flow problem was not readily available in those days. Wallis (1969) introduced the unit cell concept and asserted that it would be possible to describe the behaviour of the entire flow throughout the pipe once the behaviour of a unit cell could be pinpointed. Dukler and Hubbard (1975) and Fernandes et al (1983) developed hydrodynamic models aimed at describing the behaviour of horizontal and vertical slug flows respectively. Taitel and Barnea (1990) presented a generalized slug flow model for all pipe inclinations. In their model, both the liquid and the gas phases were supposed to be incompressible; and mass and momentum balances provided an expression for the pressure drop in the mixing zone behind the elongated bubble as a function of the friction losses along the liquid film and the geometrical profile of the elongated bubble.

The advances introduced in the digital computers during the 1990s paved the way for the development of transient slug flow models which would consider the transient behaviour of such intermittent flows. The chief transient models are the *two-fluid model*, the *drift flux model* and the *slug tracking model*. Taking the gas compressibility into account, Taitel and Barnea (1998) developed a model which considers the coalescence of neighbouring elongated bubbles. Rodrigues (2009) presented a model for the liquid film, the elongated bubble and the liquid slug based on mass and momentum balance around these regions. The gas phase is regarded as compressible and ideal.

The aforementioned models do not consider flow direction changes due to the terrain topography. Wood (1991) presented one of the pioneering studies on hilly terrain flows. Zheng et al (1994) and Al-Zafram et al (2005) reported liquid accumulation during the transit of a unit cell through an elbow at a lower pipe location (downward flow, then upward). Gravitational forces and surface tensions cause this accumulation which, by its turn, gives rise to two other phenomena: the growth of the liquid slug and the formation of a whole new one. Based on Rodrigues (2009), Barbosa Filho (2010) presented a slug flow model for the vertical-to-horizontal pipe inclination transition. Conte et al (2011) presented a work for a horizontal flow entering an upwardly inclined pipe section. According to this author, the liquid accumulation in the elbow increases the liquid slug length during its transit through the said elbow.

The present work focus on an experimental study for slug flows in a 5.6-m horizontal section followed by a 7-degree (0.1222 radians) 3.3-m inclined pipe, both with 26 mm (~1 inch) OD. This experiment was carried out at a lab facility in the premises of the Thermal Sciences Laboratory at the Federal Technological University of Paraná (UTFPR) in Curitiba, Brazil. The experimental rig is equipped with four metering stations aimed at measuring the relevant parameters of the slug flows upon their transit through these stations. A high-speed digital camera captured the splitting of the elongated bubble in the elbow whenever that phenomenon occurred. Statistical models were used to validate the recorded data.

2. EXPERIMENTAL PROCEDURES

2.1 The experimental rig

This experiment was designed and assembled at the Thermal Sciences Laboratory of the UTFPR. A schematic depiction of this facility is shown in Figure 1.
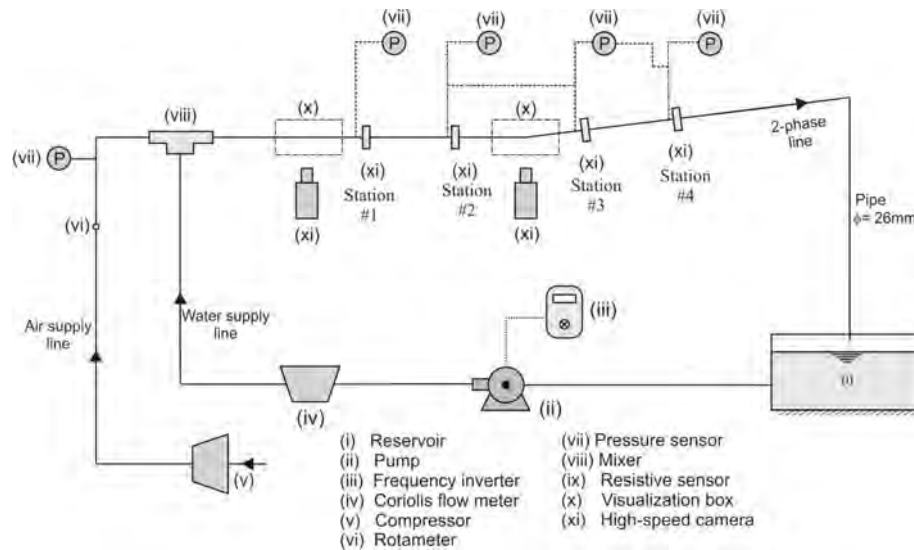
Figure 1: The experimental rig

As Figure 1 shows, air and water flow through two separate lines to the mixer, where these two phases are mixed. The resulting air-water mix leaves the mixer and is admitted into a 9.2-m length, 26-mm OD 2-phase line. The water is returned to a tank and the air is purged to the atmosphere at the end of the loop. A 30-HP centrifugal pump with a frequency inverter feeds the circuit with tap water from the 300-litre tank. Air is fed into the circuit from a 800-litre reservoir, which is pressurized by a 2-HP compressor at a maximum pressure of 0.8 MPa. Flow meters measured the flow rates of each phase before they enter the mixer. Two Coriolis flow meters for different flow rate ranges were used. The characteristics of these flow meters are shown in Table 1.

The 2-phase line consists of a 5.6-m horizontal section followed by a 7-degree (0.1222 radians) 3.3-m inclined pipe, both with 26 mm (~1 inch) OD. Four metering stations are installed along such lines, as shown in Figure 2. Pressure transducers and resistive twin-wire sensors equip each metering station. The first station (#1) is positioned at 164D

from the inlet; station #2 at 212D (shortly before the elbow); station #3 at 230D (the first in the inclined section, shortly after the elbow); and station #4 at 286D. Table 2 shows the specs of the pressure transducers.

Table 1 Flow meter characteristics

	Brand/Model	Range	Accuracy
Air	Reotest Haake/96039	70-260 l/h	±0.5%
	Reotest Haake /96044	320-3200 l/h	±0.5%
	Reotest Haake /96049	700-800 l/h	±0.5%
Water	Optimass/7300	1-10 l/s	±0.1%
	Micro Motion/F050S	0-1.5 l/s	±0.1%
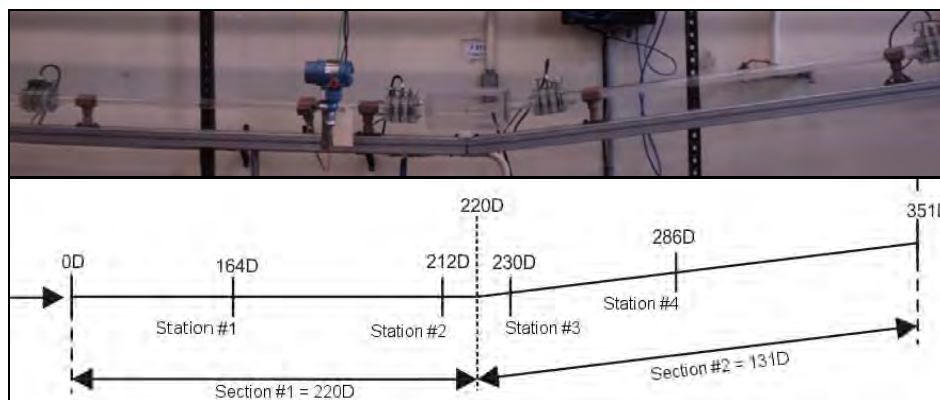
Figure 2- The experimental apparatus

Table 2 Pressure transducers' specifications

Station #	Brand/Model	Range	Accuracy
Rotameter	*Rosemount*/3051	0-150 Psi	±0.1%
1	*Rosemount*/3051	0-150 Psi	±0.1%
2	*Rosemount* /2051	0-7.5 Bar	±0.1%
3	*Rosemount* /2051	0-2.5 in H_2O	±0.1%
4	Smar/LD302	0-20 inH_2O	±0.1%

Two high-speed cameras are positioned at specific pipe locations; one shortly before stations #1 and the second right at the elbow. A network based on the FieldBus specification fetches the analogic signals from the temperature and pressure sensors, as well as from the flow meters. These signals are transferred to a PCI board that performs the required analogic-to-digital conversion. After being converted, the signals are sent to a computer for storage. A *LabView*® program entirely developed in UTFPR stores the superficial velocities of the liquid and the gas, pressures and temperatures from each metering station.

2.2 Resistive sensors

The twin-wire resistive sensors used in the experiment were entirely developed in the UTFPR instrumentation labs. Each of the four 2-phase line metering stations (see Figs. 1 and 2) has one of these sensors. Figure 3 shows how those sensors are built in the 2-phase line.

Parra, V. E. L; Cozin, C.; Barbuto, F. A. A., Amaral, C. A. F, Silva, M. J. and Morales, R. E. M.
An Experimental Study on the Development of Gas-Liquid Slug Flows with Direction Change
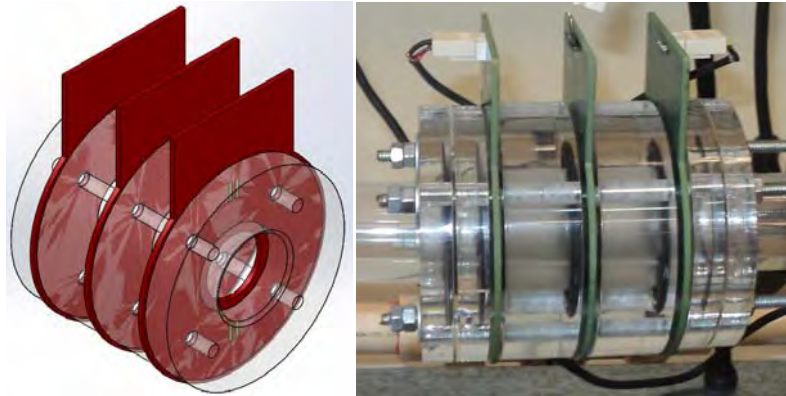
Figure 3 – Twin-wire sensor (schematics, left) and actual *in-situ* installation (direita)

Their three flanges are made of acrylic and their printed circuit boards are made of fiberglass with printed copper wiring. A ground wire connects the sensor's middle flange to the ground; that is done to prevent signal interference between the other two circuits at the extremities. The printed circuits have two stainless steel wire filaments each with 0.12 mm of diameter; the first transmits signals to the flow whereas the second captures the signal. A 1.5 kHz, 5 Vpp signal is transmitted through the fluids in motion; current reaches a maximum when the pipe is totally filled with water whereas a minimum current value is obtained when only air fills the pipe, due to water's much higher electrical conductivity.

2.3 Signal processing

The measurements from the twin-wire sensor are brought into the computer as voltage signals. A program written in LabView receives and stores these signals on a computer. From these signals, the following flow parameters must be retrieved: the void fractions, the translational velocity and the length of both the elongated bubble and the liquid slug and the slug frequency. The void fractions are indirectly inferred from the straight line correlation between the voltage measurements and the level of the liquid in the pipe. The voltage reaches its maximum value when the liquid film thickness, $H_{LB}(t)$, equals the pipe diameter and a minimum when $H_{LB}(t)$ is equal to zero. The calculation relationship between the liquid film thickness and the voltage, used to calibrate the sensors, is given by Table 3.

Table 3 – Calculation relationship between the liquid film thickness and the voltage.

Liquid film thickness	$\dfrac{H_{LB}(t)}{D} = \dfrac{V(t) - \overline{V}_{empty}}{\overline{V}_{full} - V_{full}}$
Voltage empty	$\overline{V}_{empty} = \dfrac{1}{N_t} \displaystyle\sum_{k=0}^{k=N_{t-1}} V_{full}(t)$
Voltage full	$\overline{V}_{full} = \dfrac{1}{N_t} \displaystyle\sum_{k=0}^{k=N_{t-1}} V(t)$

where $V(t)$ is the voltage as a function of time and where N_t is the size of the data sample and t is time.

Figure 4 illustrates the procedure for calculating the liquid film thickness as described above. The liquid-gas interface is represented by the variation of the signal amplitude from a value close to unity to a lower, rather constant one (or the other way around). The amplitude ≈ 1 relates to the liquid plug whereas the lowest signal amplitude represents the transit of the elongated bubble.
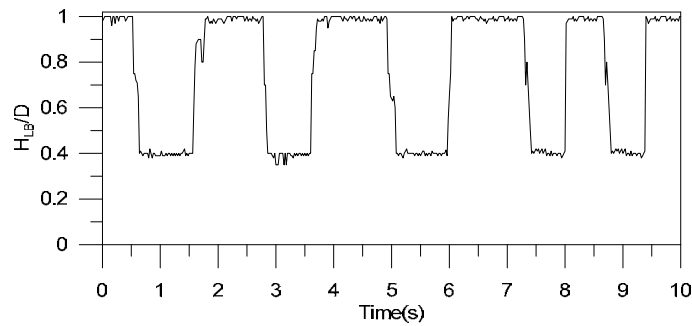
Figure 4 – Time series for the liquid level in slug flows

The geometric entities shown in Figure 5 and the relationships expressed Equations (4) and (5) are used to compute the void fraction, R_{GB},:
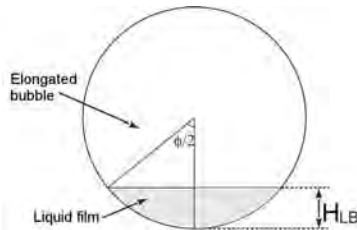
Figure 5- Liquid film thickness

$$\phi(t) = 2\arccos\left(1 - 2\frac{H_{LB}(t)}{D}\right) \qquad (4)$$

$$R_{GB}(t) = \frac{2\pi - \phi(t) + sin(\phi(t))}{2\pi} \qquad (5)$$

The signal from Sensor 1 is used to determine the length of both the liquid slug and the elongated bubble. The elongated bubble speed is calculated from the signals produced by Sensors 1 and 2. Figure 6 shows the void fraction as a function of the signals from Sensors 1 and 2.
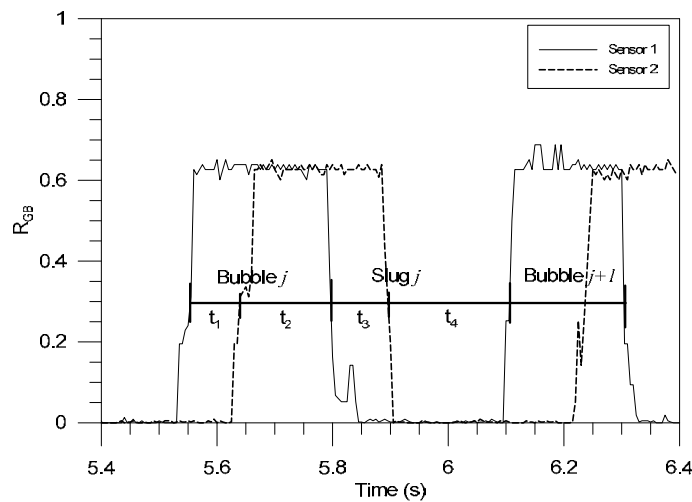
Figure 6 - Void fraction as a function of the signals from Sensors 1 and 2

The translational velocity (U_{Tj}), bubble length, slug length and bubble slug frequency are calculated according to the equations shown in Table 4:

Table 4 – Slug flow parameters

Bubble velocity	$U_{Tj} = \dfrac{\Delta L}{t_1}$
Bubble length	$L_B = U_{Tj}\left(t_1 + t_2\right)$
Slug length	$L_S = U_{Tj+1}\left(t_3 + t_4\right)$
Slug frequency	$f = \dfrac{1}{t_t} = \dfrac{1}{\left(t_1 + t_2 + t_3 + t_4\right)}$

ΔL is the distance between the circuit boards of two consecutive twin-wire sensors and t_1 is the elapsed time between the detection of the elongated bubble front by these sensors. $(t_1 + t_2)$ is the time elapsed between the detection, by the sensors, of the $(j)^{th}$ bubble nose and its rear and $(t_3 + t_4)$ is the time elapsed between the detection of the rear of the j bubble rear and the nose of the $(j+1)^{th}$ bubble.

3. RESULTS AND DISCUSSIONS

3.1 Experimental test grid

Sixteen tests for air-water slug flows were carried out. Table 5 shows the selected test grid. Liquid and gas superficial velocities, as well as the estimated bubble frequency are shown for every A@W#n point, where n is the test number. "A@W" stands for "air and water".

Table 5 – Test grid

	j_L [m/s]	j_G [m/s]	*Freq.* [Hz]
A@W#1	0.500	0.356	1.620
A@W#2	0.700	0.217	2.486
A@W#3	0.750	0.533	2.563
A@W#4	1.000	0.300	4.878
A@W#5	1.000	0.717	3.163
A@W#6	1.000	1.034	2.211
A@W#7	1.200	0.219	5.127
A@W#8	1.250	0.835	3.472
A@W#9	1.500	0.306	7.433
A@W#10	1.500	0.673	5.804
A@W#11	1.500	1.070	3.840
A@W#12	1.700	0.224	5.924
A@W#13	2.000	0.390	9.430
A@W#14	2.000	0.638	8.847
A@W#15	2.000	1.277	5.290
A@W#16	2.500	0.410	8.058

3.2 Analyses of the experiments

Equation (6) shows a model for the translation velocity of an elongated bubble (Bendiksen 1984):

$$U_T = C_0 J + C_\infty \sqrt{gD} \tag{6}$$

where U_T is the Bendiksen's translational velocity, J is the superficial velocity of the mixture C_o and C_∞ are empirical coefficients. Figure 7 shows a comparison between the translational velocities obtained during the experiments for each of the four resistive sensor stations and the values calculated by Equation (6). A high-speed camera was used to certify that the resistive sensor was accurately measuring the translational speeds. As Figure 7 shows, the difference between

the measured values and those calculated by Bendiksen's correlation lies within ±10% for the measurements taken at the four stations. Yet, some translational velocities as calculated with the aid of the high speed camera show underestimated values (below the -10% line) when compared to Bendiksen – an effect due to the inability of the image processing software to discern the nose of an elongated bubble following a highly aerated liquid slug.
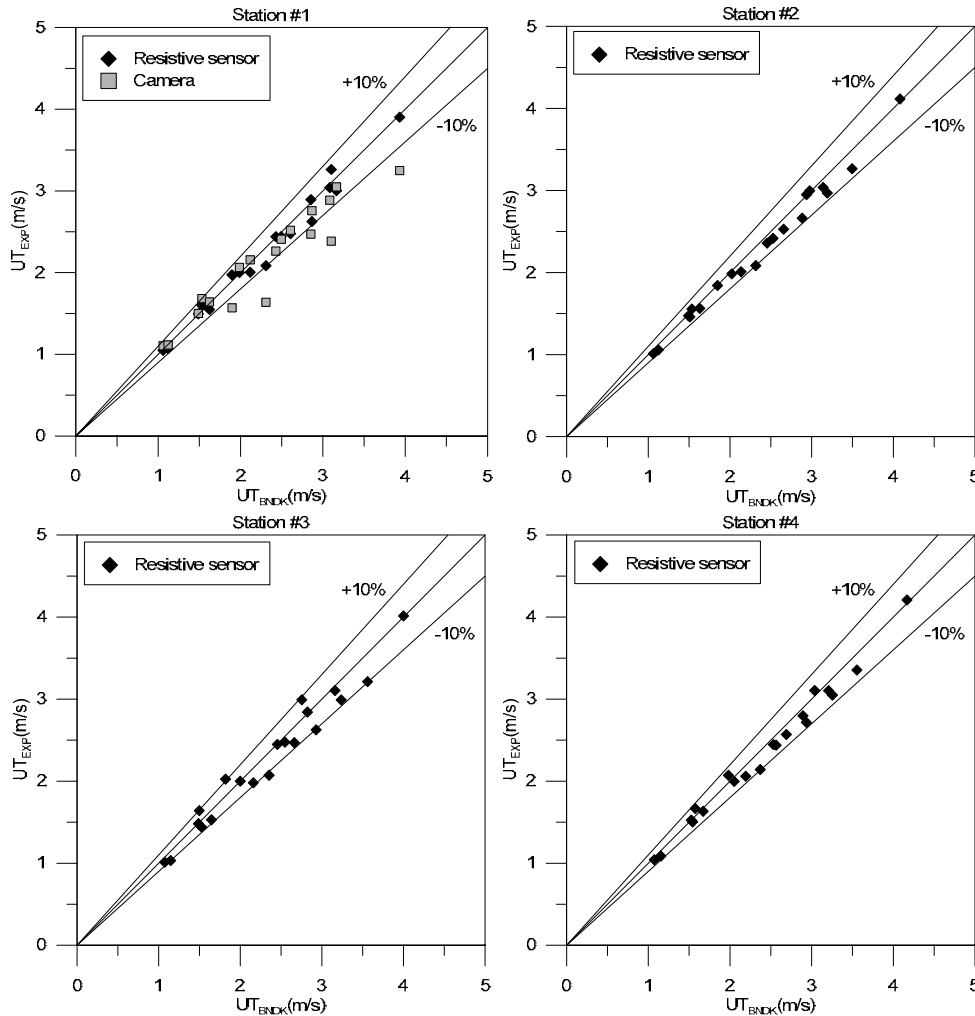
Figure 7 – The translational speed of the elongated bubbles at the four sensor stations

Similarly to the bubble translational velocity, the measured unit cell frequency was compared to correlations found in the literature and shown in Table 6.

Table 6 - Correlations for calculating the frequency of a unit cell

Correlation	Equation
Gregory e Scott (1969)	$f = 0.0226\left[\dfrac{j_L}{J}\left(\dfrac{2.02}{D}+Fr_j^2\right)\right]^{1.2}$
Heywood e Richardson (1979)	$f = 0.0434\left[\dfrac{j_L}{J}\left(\dfrac{2.02}{D}+Fr_j^2\right)\right]^{1.02}$

Where Fr_j is the Froude number and D is the pipe diameter. The dimensionless slug unit cell frequency, fD/j_G, obtained from the experiments, as well as the curves of Gregory and Scott(1969) and Heywood and Richardson(1979) correlations plotted as functions of the dimensionless number j_G/j are shown in Figure 8. These curves exhibit an

exponential trend, and for $j_G/j \geq 0.4$ a good agreement between the correlations and the experimental data is observed; otherwise the said correlations underestimate the experimental data values obtained from the four sensor stations. As it can be seen, the frequency is inversely proportional to j_G/j, increasing with the decrease of this dimensionless number and decreasing otherwise. In general, experiments and correlations showed a fair agreement.
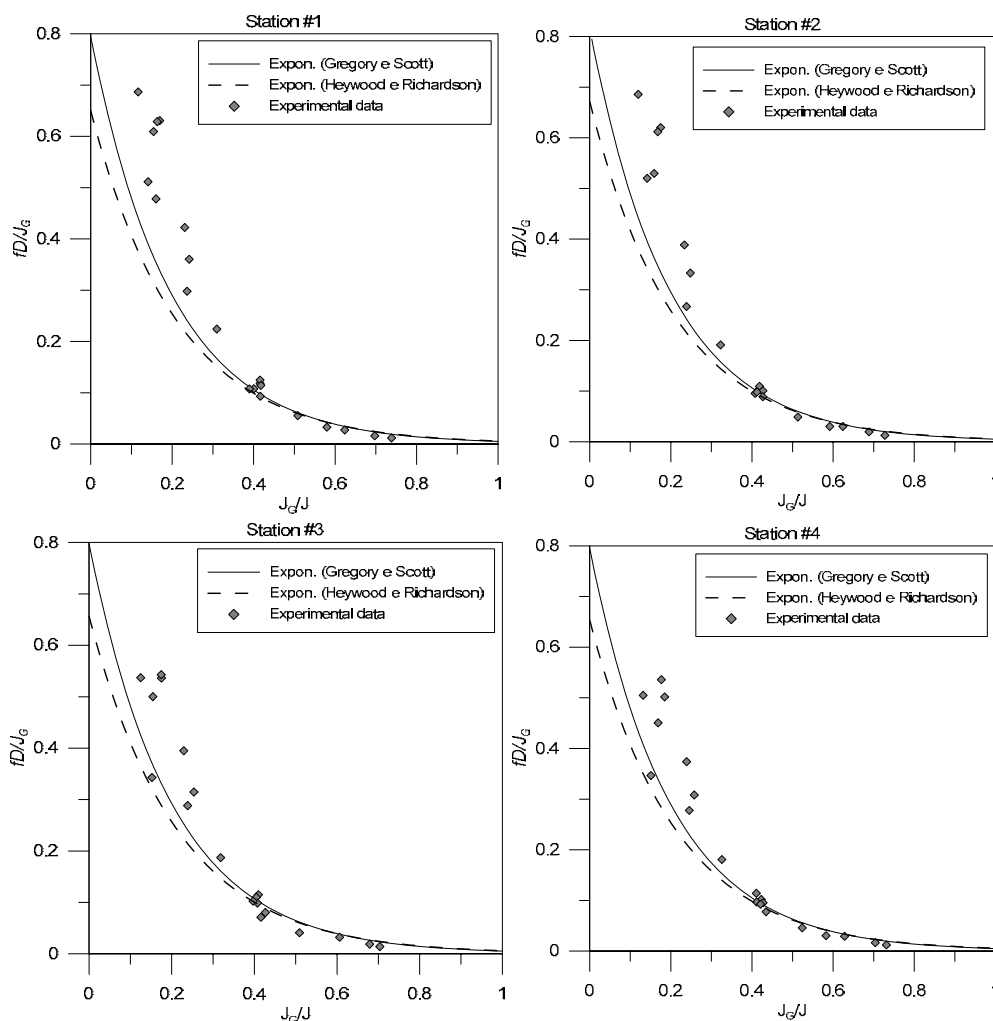
Figure 8 – Unit cell frequencies at the four sensor stations

Figures 9 and 10 show averaged experimental results for test cases A@W#1 and A@W5. The dots represent the four sensor stations. The charts show the evolution of the lengths of the elongated bubble, the elongated bubble translational speed and the local pressure at each station. The variations in the lengths of the elongated bubble and the liquid slug are directly linked to bubble coalescence and liquid accumulation in the elbow, respectively. The latter phenomenon is responsible for the generation of a new liquid slug and the growth of the preceding one.

A reduction in the average elongated bubble length between stations 3 and 4 can be observed in Figure 9. This effect is due to the bubble break-up. An increase of the liquid slug length is shown in Figure 10. This happens when the elongated bubble flows past the elbow, thus increasing its speed and thence increasing the length of the liquid slug.

Both figures show an increase in the length of the elongated bubble and the liquid slug between stations 1-2 and 3-4. That is due to coalescence, a phenomenon arising from the fusion of two neighbour cells to form a single one.
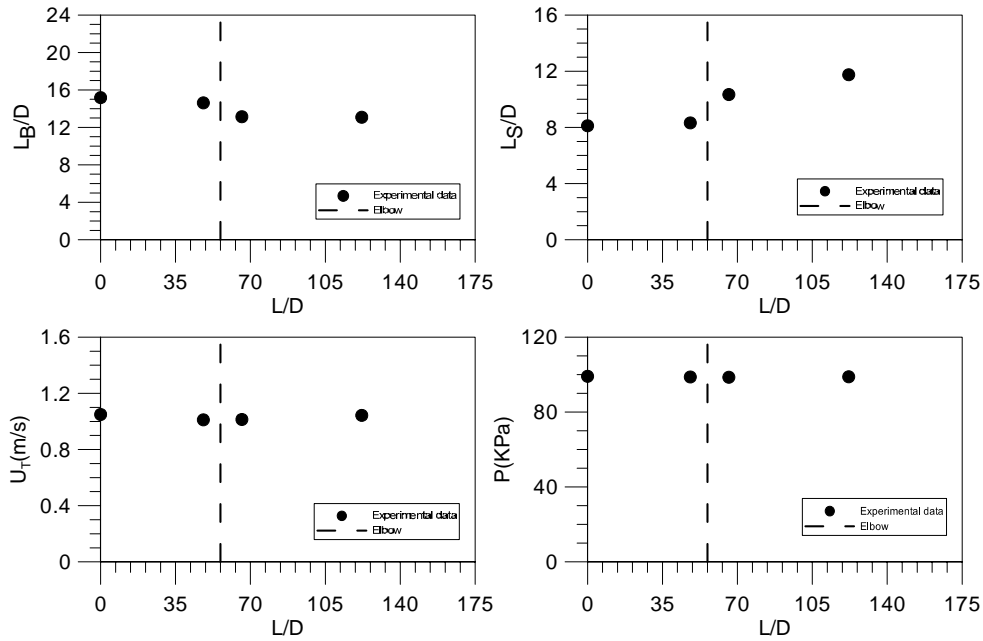
Figure 9 – Averaged results for bubble and slug length, bubble velocity and for pressure drop at A@W#1
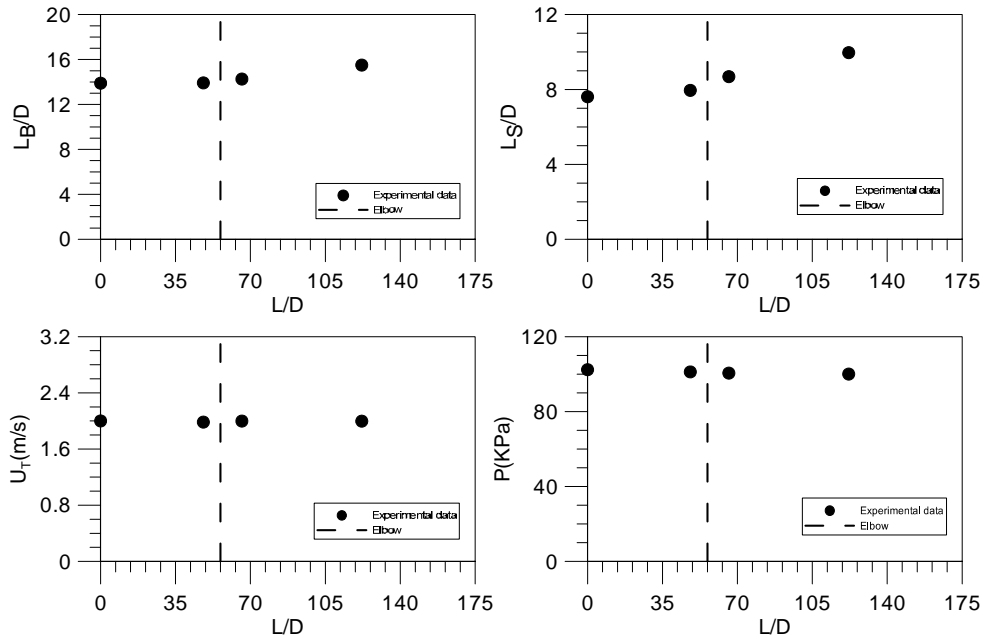
Figure 10 – Averaged results for bubble and slug length, bubble velocity and for pressure drop at A@W#5

Figures 11 and 12 show the probability density functions (PDF) for the length and translational speed of the elongated bubble and for the liquid slug length from tests A@W#1 and A@W#5 at sensor stations 2, 3 and 4.

Parra, V. E. L; Cozin, C.; Barbuto, F. A. A., Amaral, C. A. F, Silva, M. J. and Morales, R. E. M.
An Experimental Study on the Development of Gas-Liquid Slug Flows with Direction Change
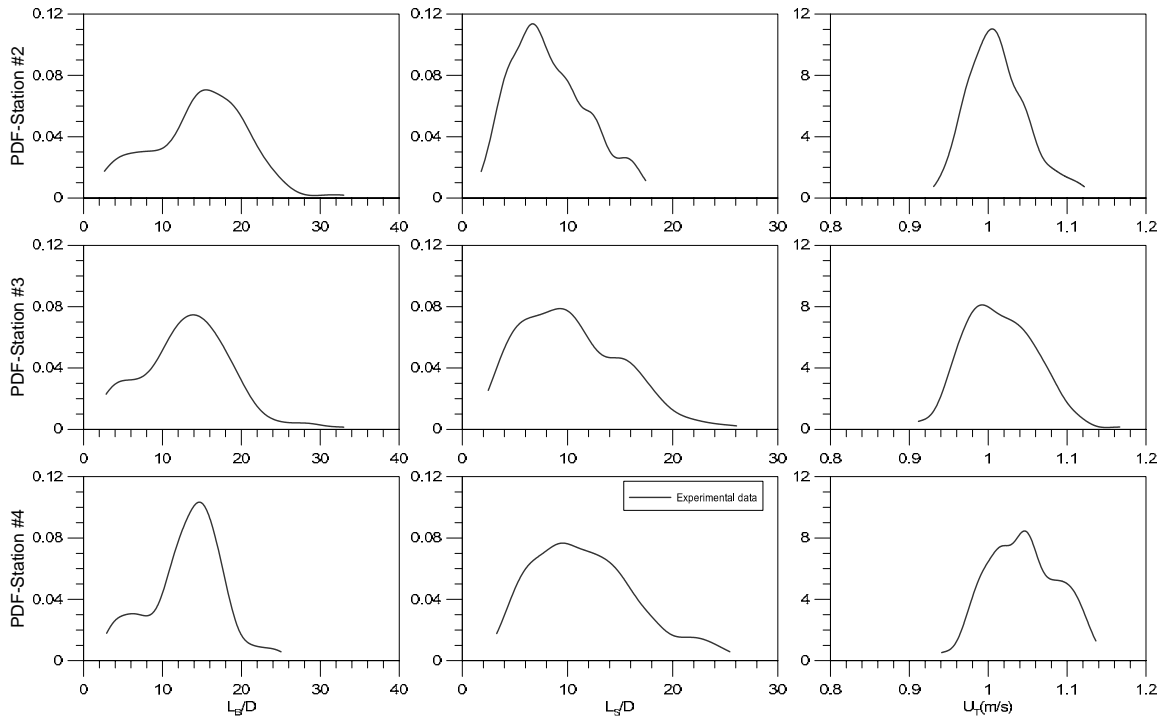
Figure 11 – PDFs for A@W#1
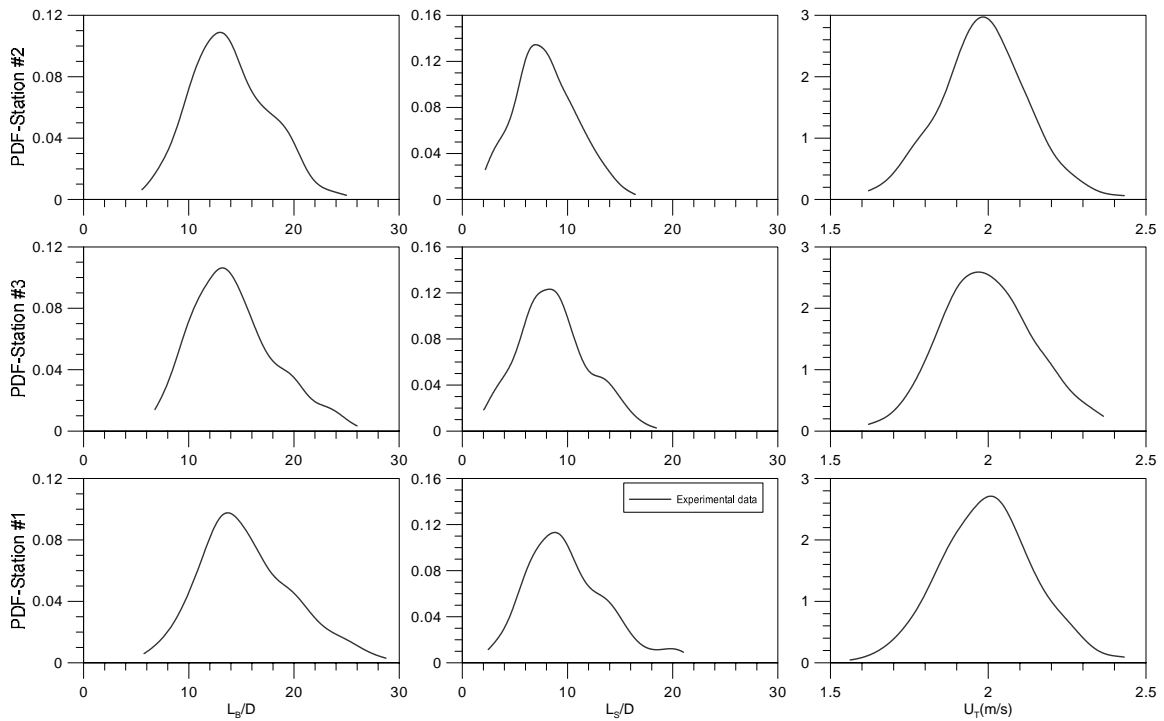
Figure 12 – PDFs for A@W#5

3.3 Analysis of flow footage shot at the elbow

The main objective of filming the flow at the elbow is to certify that a bubble break-up really occurred. Figure 13 shows the division of an elongated bubble. In frame (a), the central region of a bubble is right at the elbow on its way to the 7-degree upward section. In (b), the bubble stretches quite remarkably whilst the liquid film thickness increases. In (c), the elongated bubble has just broken and, finally, frame (d) shows the break-up process after its completion.
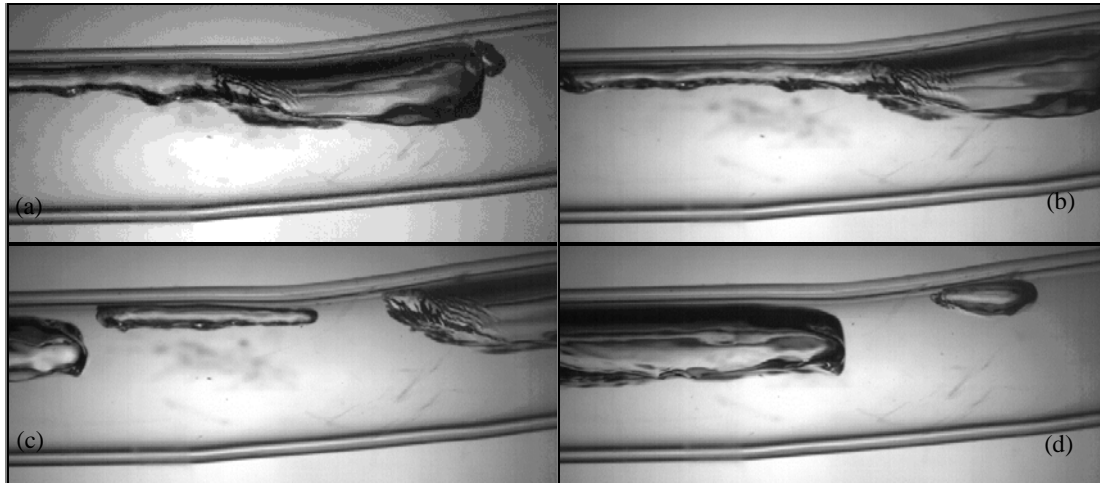
Figure 13- Frames depicting the break-up of an elongated bubble in the elbow: test case A@W#1

The bubble break-up takes place in accordance to the Kelvin-Helmholtz's (K-H) instability criterion. Such instability is due to flow perturbations between the liquid and gas layers when the bubble flows through the elbow. Surface tensions and gravitational forces initiate this kind of perturbation. The motion of the two fluid layers gives rise to a suction force over the wave due to the Bernoulli effect, which tends to divide the elongated bubble. That explains the increase in the in-situ pressure from station 3 to 4 during the split-up of the bubble.

For all the tests in the grid, only A@W#1 showed bubble split-up. In most of the other tests, the pressure drop from station to station is positive. Test A@W#1 is an exception.

4. CONCLUSIONS

The translational velocity of the elongated bubble and the slug frequency obtained with resistive sensors were matched to correlations in the literature, and a good agreement was found.

The break-up of the elongated bubbles in the elbow produce a decrease in their average length between stations 2 and 3. The high-speed camera captured the break-up of elongated bubbles in the elbow for test case A@W#1. The break-up is observed whenever the average bubble lengths decrease during their transit through the elbow and the subsequent change in direction.

An increase in the liquid slug between sensor stations 2 and 3 was observed. This increase could be explained on the grounds of either the coalescence of the elongated bubbles or the increase in the liquid slug length as a consequence of the accumulation of liquid in the elbow.

The growth of both the liquid slug and the elongated bubble lengths between stations 1-2 and 3-4 is due to the coalescence of the elongated bubbles.

5. REFERENCES

Al-Safran, E. M., Sarica, C., Zhang, H., & Brill, J. (2005). Investigation of slug flow characteristic in valley of a hilly terrain pipeline. International Journal of Multhiphase Flow, 31, 337-357.

Barbosa, F. (2010). Estudo do escoamento bifásico padrão golfadas de líquido na transição vertical ascendente-horizontal utilizando um modelo slug-tracking. Universidade Estadual de Campinas, Campinas.

Bendiksen, K. (s.d.). An Experimental Investigation of the Motion of Long Bubbles in Inclined Tubes. *International Journal of Multiphase Flow, 10*(4), 467-483.

Conte, M. G., Bassani, C. L., Perea Medina, C., Scorsim, Ó. B., do Amaral, C. E., & Morales, R. E. (2011). Numerical analysis of slug flow for slight changes of direction using slug tracking model. *CILAMCE*.

Parra, V. E. L; Cozin, C.; Barbuto, F. A. A., Amaral, C. A. F, Silva, M. J. and Morales, R. E. M.
An Experimental Study on the Development of Gas-Liquid Slug Flows with Direction Change

Dukler, A. E., & Hubbard, M. G. (1975). A model for gas-liquid slug flow in horizontal and nearhorizontal tubes. *Ind. Eng. Chem. Fundam., 14*(4), 337-347.

Fernandes, R. C. (1983). Hydrodynamic model for gás-liquid slug flow in vertical tubes. *American Institute for Chemical Engineers Journal, 29*(6), 981-989.

Rodrigues, H. (2009). *Simulação númerica do escoamento bifásico gás líquido no padrão de golfadas utilizando um modelo lagrangeano de seguimento de pistões.* Universidade Tecnológica Federal do Paraná, Curitiba.

Taitel, Y., & Barnea, D. (1990a). Two phase slug flow. *Advances in Heat Transfer, Harnett J. P. and Irvine Jr. T. F., 20*, 83-132.

Taitel, Y., & Barnea, D. (1990b). A consistent approach for calculating pressure drop in inclined slug flow. *Chemical Engineering Science, 45*(5), 199-1206.

Taitel, Y., & Barnea, D. (1998). Effect of gas compressibility on a slug tracking model. *Chemical Engineering Science, 53*(11), 2089-2097.

Wallis, G. B. (1969). *One dimensional-two-phase flow*. New York: McGraw-Hil.

Wood, D. (1991). Mechanistic modeling of terrain-induced slugs in gas/condensate lines. *In: Proccedings of BHRG Multiphase Conference*.

Zheng, G., Brill, J., & Taitel, Y. (1994). Slug flow behavior in a hily terrain pipeline. *International Journal Multiphase Flow, 20*(1), 63-79.

6. RESPONSIBILITY NOTICE

The author(s) is (are) the only responsible for the printed material included in this paper.